Three-charged-particle systems in the framework of coupled coordinate-space few-body equations

Renat A. Sultanov [*]
Department of Mathematics, Odessa College, 201 W. University Boulevard, Odessa, Texas 79764, USA

Sadhan K. Adhikari [†]
Instituto de Física Teórica, UNESP–Universidade Estadual Paulista, 01140-070 São Paulo, São Paulo, Brazil

(Received 22 February 2023; accepted 30 May 2023; published 30 June 2023)

We study *three-charged-particle* low-energy elastic collision and particle-exchange reactions with special attention to the systems with Coulomb interaction and an additional nuclear interaction employing a close-coupling expansion scheme to a set of coupled two-component few-body equations. First we apply our formulation to compute low-energy elastic scattering phase shifts for the $d + (t\mu^-)_{1s}$ collision, which is of significant interest for the muon-catalyzed-fusion D-T cycle. Next, we study the particle-exchange reaction $d + (pX^-) \to p + (dX^-)$ with the long-lived elementary heavy lepton stau X^- which can play a critical role in the understanding of the big-bang nucleosynthesis and the nature of dark matter. We also study the total cross sections and rates for two-particle-exchange reactions involving antiprotons ($\bar{p}$), deuterons (d), and tritons (t), e.g., $\bar{p} + (d\mu^-)_{1s} \to (\bar{p}d)_{1s} + \mu^-$ and $\bar{p} + (t\mu^-)_{1s} \to (\bar{p}t)_{1s} + \mu^-$, where μ^- is a muon. The effect of the final state short-range strong $(\bar{p}d)$ and $(\bar{p}t)$ nuclear interactions is significant in these reactions, which increases the reaction rates by a factor of ≈3.

DOI: 10.1103/PhysRevC.107.064003

I. INTRODUCTION

Quantum-mechanical few-body systems play an important role in different fields of physics. This is true in the case of atomic-molecular physics, chemical, nuclear, and particle physics [1] and also in the case of condensed matter physics [2]. Therefore, special methods and techniques to handle quantum-mechanical few-body problems have emerged as an important area of research [3,4]. The fundamental difference between a two-body and a few-body process is that in a few-body process the two-body scattering can occur off the energy shell (off-shell) and can probe the off-shell part of two-body interaction which is not accessible in a two-body process.

In this paper we develop a close-coupling expansion scheme to a set of coupled two-component scattering equations to study elastic collision and particle-exchange reactions involving three charged particles. These numerical schemes are usually tested in atomic systems with only Coulomb interaction, such as electron-hydrogen and positron-hydrogen systems. We apply this procedure to the study of collisions in a few three-body atomic systems with Coulomb plus nuclear interactions, which are of particular importance in physics from both experimental and theoretical points of view. This investigation into three-body systems may shed light on our knowledge about nuclear interactions. The effect of final-state strong nuclear interaction on the collisions in these three-body systems is found to be significant.

As the first application to our approach we study the elastic collision

$$d + (t\mu^-)_{1s} \to (t\mu^-)_{1s} + d, \tag{1}$$

where d (t) represents a deuteron (triton) and μ^- a muon below the $n = 2$ threshold of $(t\mu^-)$, which is of significant interest for the muon-catalyzed-fusion cycle in a cold liquid hydrogen (DT) environment [5–7]. This collision is a quite challenging three-body process especially at low-energies due to the long-range d-$(t\mu)$ polarization interaction. We compare our numerical results for phase shifts at different energies with those of other calculations.

Next we study the following particle-exchange reaction and elastic collision:

$$\begin{aligned} d + (pX^-) &\to (pX^-) + d \\ &\searrow (dX^-) + p, \end{aligned} \tag{2}$$

where p represents a proton, d represents a deuteron and X^- the long-lived heavy negatively charged lepton stau. The stau particle can play a critical role in the understanding of the big-bang nucleosynthesis (BBN) [8,9] and the nature of dark matter. We compare our total cross sections for these processes with the results of Ref. [10]. The lepton X^- is a supersymmetric (SUSY) partner of the τ lepton with an estimated mass of about ≈125 GeV [11]. Experimental search for this particle is still ongoing [11–14]. It is interesting to note that the quasistable X^- can make Coulomb bound states with nuclei and could severely affect the early BBN era nuclear reactions through a so called X^--catalyzed process [15–17]. In the contemporary literature this phenomenon has been named the catalyzed big-bang nucleosynthesis (CBBN). In some

[*] rsultanov@odessa.edu; r.sultanov2@yahoo.com
[†] sk.adhikari@unesp.br; https://professores.ift.unesp.br/sk.adhikari/

senses CBBN is similar to the processes of muon catalyzed fusion [5,18], when μ^- effectively shields the Coulomb fields of nuclei and increases the rates of nuclear reactions. The idea of cold catalysis or fusion of nuclear reactions between hydrogen isotopes dates back to early works in particle physics in the 1940s, and the first works related to the X^- catalysis have their origins in the late 1980s and the early 1990s [10,19–21]. For example, in Ref. [10] paths to observation of X^- were numerically estimated.

The particle-exchange reactions

$$\bar{p} + (d\mu^-)_{1s} \to (\bar{p}d)_\alpha + \mu^-, \tag{3}$$

$$\bar{p} + (t\mu^-)_{1s} \to (\bar{p}t)_\alpha + \mu^-. \tag{4}$$

considered next involving antiproton $\bar{p}$ are specially significant because these few-body processes with $\bar{p}$ will provide information about its interaction with elementary hadrons such as deuterons, tritons, etc. [22–27]. In Eqs. (3) and (4) α $(\equiv nl)$ denotes the nl bound state of $(\bar{p}d)$ or $(\bar{p}t)$, e.g., $(\bar{p}d)_{nl}$ or $(\bar{p}t)_{nl}$. A slow $\bar{p}$ can approach muonic atoms at a very short distance without annihilation followed by a three-body reaction to form an antiprotonic hydrogen atom. This situation is quite similar to well-known muon-catalyzed fusion reactions, where a negative muon μ^- binds, for example, d and tritium t nuclei so close and so strongly that the nuclear reaction $d + t$ occurs with a high probability [18]. Therefore, low-energy few-body systems can be useful to study nuclear forces and annihilation processes between a proton and an antiproton. These reactions were studied before using adiabatic [28] and nonadiabatic [29] approaches. We would like to emphasize here that the knowledge of the antimatter-matter $(\bar{N}N)$ strong interaction is of significant importance in nuclear physics [30]. In Refs. [31,32] it was pointed out that muonic atoms can be especially useful to study nuclear properties.

In recent years research in the field of low-energy antiproton and antihydrogen physics has gained significant momentum [33–36]. Primarily, this is connected with the creation and confinement of cold antihydrogen atoms $\bar{H}$ and with the detection of $^{3(4)}\mathrm{He}^+$ $\bar{p}$ few-body systems, i.e., metastable antiprotonic helium atomcules [37]. Also, currently of a special interest are different few-particle systems and collisions with participation of antiprotons and antihydrogen atoms [38,39], and muonic atoms [40–44]. Another strong motivation of the antihydrogen and antimatter physics research is to check and confirm certain fundamental laws, like the charge conjugation, parity, and time reversal (CPT) symmetry of quantum electrodynamics [45,46].

To correctly evaluate reactions (2)–(4) and the low-energy elastic scattering process (1) we adopt a general few-body approach based on a decomposition of the total three-body quantum-mechanical wave function $|\Psi\rangle$ on two special components $|\Psi_1(\vec{r_{23}}, \vec{\rho_1})\rangle$ and $|\Psi_2(\vec{r_{13}}, \vec{\rho_2})\rangle$. Each component describes a specific spatial configuration in the three-body system. The few-body method was developed in the series of papers; see for example [47–53]. We also would like to add here that this approach allows us to correctly include final-state interactions in various atomic and nuclear few-body reactions [53].

In Sec. II we present the few-body approach together with the inclusion of the final-state nuclear interaction in the case of the reactions (3) and (4). All our numerical results, namely for processes (3) and (4), for the elastic scattering muonic process (1), and for the p-d exchange collision (2), are given and discussed in Sec. III. Conclusions are given in Sec. IV. The corresponding procedure to obtain a set of one-dimensional integral-differential equations together with the appropriate boundary conditions is presented in the Appendix. Muonic atomic units (m.a.u.) are used in this work, i.e., $m_\mu = e^- = \hbar = 1$, where m_μ is the muon mass, e^- is the charge of an electron, and $\hbar$ is Planck's constant.

II. COUPLED FEW-BODY EQUATIONS IN COORDINATE SPACE

In this work we deal with elastic and rearrangement scattering at low energies below the three-body breakup threshold with Coulomb three-body systems with arbitrary unequal masses. In all the processes we consider there are only two bound partitions. Hence below the three-body breakup threshold only two two-cluster asymptotic configurations are possible in the three-body system, e.g., $(23) - 1$ and $(13) - 2$ being determined by their own Jacobi coordinates $\{\vec{r}_{j3}, \vec{\rho}_k\}$:

$$\vec{r}_{j3} = \vec{r}_3 - \vec{r}_j, \quad \vec{\rho}_k = \frac{m_3\vec{r}_3 + m_j\vec{r}_j}{m_3 + m_j} - \vec{r}_k \quad (j \neq k = 1, 2). \tag{5}$$

Here $\vec{r}_j, m_j$ are the coordinates and the masses of the particles $j = 1, 2, 3$ respectively. This suggests a two-cluster formulation which uses only two components.

A general procedure to derive such formulations is described in Refs. [48,49,53]. In this approach the three-body wave function is represented as follows:

$$|\Psi\rangle = \Psi_1(\vec{r}_{23}, \vec{\rho}_1) + \Psi_2(\vec{r}_{13}, \vec{\rho}_2), \tag{6}$$

where each wave function component is determined by its own Jacobi coordinates. Moreover, $\Psi_1(\vec{r}_{23}, \vec{\rho}_1)$ is quadratically integrable over the variable $\vec{r}_{23}$, and $\Psi_2(\vec{r}_{13}, \vec{\rho}_2)$ over the variable $\vec{r}_{13}$. The Schrödinger equation for the three-body system

$$(E - \hat{H}_0 - V_{12} - V_{23} - V_{31})|\Psi\rangle = 0, \tag{7}$$

can be identically rewritten as a set of two coupled equations for the components $|\Psi_1\rangle$ and $|\Psi_2\rangle$:

$$[E - \hat{H}_0 - V_{23}(\vec{r}_{23})]\Psi_1(\vec{r}_{23}, \vec{\rho}_1) = [V_{23}(\vec{r}_{23}) + V_{12}(\vec{r}_{12})]\Psi_2(\vec{r}_{13}, \vec{\rho}_2), \tag{8}$$

$$[E - \hat{H}_0 - V_{13}(\vec{r}_{13})]\Psi_2(\vec{r}_{13}, \vec{\rho}_2) = [V_{13}(\vec{r}_{13}) + V_{12}(\vec{r}_{12})]\Psi_1(\vec{r}_{23}, \vec{\rho}_1). \tag{9}$$

Here, $\hat{H}_0$ is the kinetic energy operator of the three-particle system, $V_{ij}(\vec{r}_{ij})$ are Coulomb potentials between particles i and j $(i \neq j = 1, 2, 3)$, and E is the total energy. For energies below the three-body breakup threshold, Eqs. (8) and (9) exhibit the same advantages as detailed few-body

equations because they are formulated for the wave function components with the correct physical asymptotes. To solve Eqs. (8) and (9) a close-coupling method is applied, which leads to an expansion of the wave function components $|\Psi_j\rangle$ into eigenfunctions of the subsystem (target) Hamiltonians, providing one with a set of one-dimensional integral-differential equations after partial-wave projection. A further advantage of the method is the fact that the wave-function components are smoother functions of the coordinates than the total wave function.

In processes (1) and (2), the mesic atoms $(t\mu^-)$, (pX^-), and (dX^-) are bound solely by atomic interaction, and Eqs. (8)–(9) are appropriate to study these processes. However, in the case of the reactions (3) and (4) it would be necessary to explicitly include the final state nuclear interaction between the hadrons $\bar{p}$ and d in (3) and $\bar{p}$ and t in (4). Therefore, for this purpose we rewrite Eqs. (8) and (9) as follows [53]:

$$[E - \hat{T}_{\rho_1} - \hat{h}_{23}(\vec{r}_{23})]\Psi_1(\vec{r}_{23}, \vec{\rho}_1) = [V_{23}(\vec{r}_{23}) + V_{12}(\vec{r}_{12})]\Psi_2(\vec{r}_{13}, \vec{\rho}_2), \tag{10}$$

$$\left[E - \hat{T}_{\rho_2} - \hat{h}_{13}^{\bar{N}N}(\vec{r}_{13})\right]\Psi_2(\vec{r}_{13}, \vec{\rho}_2) = [\tilde{\mathbf{V}}_{13}(\vec{r}_{13}) + V_{12}(\vec{r}_{12})]\Psi_1(\vec{r}_{23}, \vec{\rho}_1), \tag{11}$$

where $\tilde{\mathbf{V}}_{13}(\vec{r}_{13}) = V_{13}(\vec{r}_{13}) + v_{13}^{\bar{N}N}(\vec{r}_{13})$, and $\hat{h}_{23}(\vec{r}_{23}) \equiv \hat{T}_{\vec{r}_{23}} + V_{23}(\vec{r}_{23})$ and $\hat{h}_{13}^{\bar{N}N}(\vec{r}_{13}) \equiv \hat{T}_{\vec{r}_{13}} + V_{13}(\vec{r}_{13}) + v_{13}^{\bar{N}N}(\vec{r}_{13})$ are the two-particle target Hamiltonians; in $\hat{h}_{13}^{\bar{N}N}(\vec{r}_{13})$ and in $\tilde{\mathbf{V}}_{13}(\vec{r}_{13})$ an additional strong $\bar{p}d$ (or $\bar{p}t$) final-state nuclear potential, viz., Eqs. (3) and (4), $v_{13}^{\bar{N}N}(\vec{r}_{13})$ has been included, where N and $\bar{N}$ represent d and $\bar{p}$ or t and $\bar{p}$. In writing Eqs. (10) and (11) we have used the identities $\hat{H}_0 \equiv \hat{T}_{\rho_1} + \hat{T}_{\vec{r}_{23}} \equiv \hat{T}_{\rho_2} + \hat{T}_{\vec{r}_{13}}$, where $\hat{T}_{\vec{r}_{ij}}$ is the kinetic energy of the pair ij and $\hat{T}_{\rho_k}$ $(i \neq j \neq k)$ is the kinetic energy of the particle k relative to the pair ij.

In order to solve Eqs. (10) and (11) a modified close-coupling approach is used. We use an expansion of the wave function components $|\Psi_1\rangle$ and $|\Psi_2\rangle$ in discreet bound-state eigenfunctions $\varphi_\alpha^{(1)}(\vec{r}_{23})$ and $\varphi_{\alpha'}^{(2)\bar{N}N}(\vec{r}_{13})$ of the subsystem (target) Hamiltonians $\hat{h}_{23}(\vec{r}_{23})$ and $\hat{h}_{13}^{\bar{N}N}(\vec{r}_{13})$, with coefficients $f_\alpha^{(1)}(\vec{\rho}_1)$ and $f_{\alpha'}^{(1)}(\vec{\rho}_2)$ respectively:

$$\Psi_1(\vec{r}_{23}, \vec{\rho}_1) \approx \sum_\alpha f_\alpha^{(1)}(\vec{\rho}_1)\varphi_\alpha^{(1)}(\vec{r}_{23}), \tag{12}$$

$$\Psi_2(\vec{r}_{13}, \vec{\rho}_2) \approx \sum_{\alpha'} f_{\alpha'}^{(2)}(\vec{\rho}_1)\varphi_{\alpha'}^{(2)\bar{N}N}(\vec{r}_{13}). \tag{13}$$

In Eqs. (12) and (13) we carry out summation over the discreet atomic bound states $\varphi_\alpha^{(1)}(\vec{r}_{23})$ and $\varphi_{\alpha'}^{(2)\bar{N}N}(\vec{r}_{13})$ included in the approximation. In reactions (3) and (4), the function $\varphi_{\alpha'}^{(2)\bar{N}N}(\vec{r}_{13})$ has the contribution of the additional nuclear interaction between $\bar{p}$ and d or $\bar{p}$ and t. The coupled few-body equations (10)–(11) will guarantee that the one-dimensional unknown coefficients $f_\alpha^{(1)}(\vec{\rho}_1)$ and $f_{\alpha'}^{(2)}(\vec{\rho}_2)$ will have correct physical asymptotes. This procedure reduces Eqs. (10) and (11) to a set of coupled one-dimensional integral-differential equations for $f_\alpha^{(1)}(\vec{\rho}_1)$ and $f_{\alpha'}^{(2)}(\vec{\rho}_2)$ after partial-wave projection [54]:

$$\left[\left(k_n^{(1)}\right)^2 + \frac{\partial^2}{\partial\rho_1^2} - \frac{\lambda(\lambda+1)}{\rho_1^2}\right]f_\alpha^{(1)}(\rho_1) = g_1 \sum_{\alpha'} \frac{\sqrt{(2\lambda+1)(2\lambda'+1)}}{2L+1} \int_0^\infty d\rho_2 f_{\alpha'}^{(2)}(\rho_2) \int_0^\pi d\omega \sin(\omega) R_{nl}^{(1)}(|\vec{r}_{23}|) \times \left[-\frac{1}{|\vec{r}_{23}|} + \frac{1}{|\vec{r}_{12}|}\right] R_{n'l'}^{(2)}(|\vec{r}_{13}|)\rho_1\rho_2 \times \sum_{mm'} D_{mm'}^L(0,\omega,0) C_{\lambda 0 lm}^{Lm} C_{\lambda' 0 l'm'}^{Lm'} Y_{lm}^*(\nu_1,\pi) Y_{l'm'}(\nu_2,\pi), \tag{14}$$

$$\left[\left(k_n^{(2)}\right)^2 + \frac{\partial^2}{\partial\rho_2^2} - \frac{\lambda'(\lambda'+1)}{\rho_2^2}\right]f_{\alpha'}^{(2)}(\rho_2) = g_2 \sum_{\alpha} \frac{\sqrt{(2\lambda+1)(2\lambda'+1)}}{2L+1} \int_0^\infty d\rho_1 f_\alpha^{(1)}(\rho_1) \int_0^\pi d\omega \sin(\omega) R_{n'l'}^{(2)}(|\vec{r}_{13}|) \times \left[-\frac{1}{|\vec{r}_{13}|} + \frac{1}{|\vec{r}_{12}|}\right] R_{nl}^{(1)}(|\vec{r}_{23}|)\rho_2\rho_1 \times \sum_{mm'} D_{mm'}^L(0,\omega,0) C_{\lambda 0 lm}^{Lm} C_{\lambda' 0 l'm'}^{Lm'} Y_{l'm'}^*(\nu_2,\pi) Y_{lm}(\nu_1,\pi). \tag{15}$$

Here $\alpha = nl$, $\alpha' = n'l'$, $g_k = 4\pi M_k/\gamma^3$ $(k = 1, 2)k_n^{(i)} = \sqrt{2M_i(E - E_n^{(j)})}$, with $M_i^{-1} = m_i^{-1} + (m_3 + m_j)^{-1}$, $E_n^{(j)}$ is the binding energy of $(j3)$, $i \neq j = 1, 2$, $\gamma = 1 - m_k m_j/[(m_3 + m_k)(m_3 + m_j)]$, $D_{mm'}^L(0, \omega, 0)$ is the Wigner function, $C_{\lambda 0 lm}^{Lm}$ is the Clebsh-Gordon coefficient [55], L is the total angular momentum of the three-body system, $\alpha = (nl\lambda)$ are quantum numbers of a three-body state, ω is the angle between the Jacobi coordinates $\vec{\rho}_i$ and $\vec{\rho}_{i'}$, ν_i is the angle between $\vec{r}_{i'3}$ and $\vec{\rho}_i$, $\nu_{i'}$ is the angle between $\vec{r}_{i3}$ and $\vec{\rho}_{i'}$, and $R_{nl}^{(1)}(|\vec{r}_{23}|)$ and $R_{n'l'}^{(2)}(|\vec{r}_{23}|)$ are the radial parts of the wave functions $\varphi_n^{(1)}(\vec{r}_{23})$ and $\varphi_{n'}^{(2)\bar{N}N}(\vec{r}_{13})$. The following relations are useful for a numerical treatment: $\sin\nu_i = (\rho_{i'}/\gamma r_{i'3})\sin\omega$ and $\cos\nu_i = (1/\gamma r_{i'3})(\beta_i\rho_i + \rho_{i'}\cos\omega)$ $(i \neq i' = 1, 2)$. Equations (14) and (15), involving smoother unknown functions $f_n^{(1)}(\vec{\rho}_1)$ and $f_{n'}^{(2)}(\vec{\rho}_2)$, are more appropriate for numerical treatment than the full three-body equations (10)–(11).

Coupled integral-differential equations (14) and (15) can be solved in the framework of different close-coupling approximation schemes, such as $2\times(1s)$, $2\times(1s+2s)$, $2\times(1s+2s+2p)$, etc. Symbol "$2\times$" indicates that the close-coupling expansion is carried out for the two wave-function components, viz., Eqs. (12) and (13). For instance, if $n=n'=1$ we apply only two atomic states, i.e., two ground states ($1s$) of each target. When $n=n'=2$ we use two or three atomic target states resulting in $2\times(1s+2s)$ or $2\times(1s+2s+2p)$ approximation. Our computing approach for numerical solution of the coupled integral-differential equations (14)–(15) is discussed in the Appendix.

The full potentials between $\bar{p}$ and d and between $\bar{p}$ and t are complex, because their second part, $v_{13}^{\bar{N}N}(\vec{r}_{13})$, possesses the asymmetric $\bar{N}$-N nuclear interactions [56–61]. In this work we did not explicitly include the strong interaction in our calculations, that is why in the case of the target $\bar{p}d$ and $\bar{p}t$ eigenfunctions we use pure two-body Coulomb (atomic) wave functions.

$$\varphi_{n'}^{(2)\bar{N}N}(\vec{r}_{13})\approx\sum_{l'm'}R_{n'l'}^{(2)}(r_{13})Y_{l'm'}(\hat{r}_{13}), \tag{16}$$

where the function $R_{n'l'}^{(2)}(r_{13})$ and the spherical harmonic $Y_{l'm'}(\hat{r}_{13})$ are the radial and the angular parts of the hydrogen-like atomic wave function [62], and $\{n',l',m'\}$ are the usual principal and the angular quantum numbers of the antiprotonic hydrogen atom. Nonetheless, the strong $\bar{p}d$ and $\bar{p}t$ interactions are approximately taken into account through the eigenenergies $\mathcal{E}_{n'}$ which have shifted values from the original Coulomb levels $\varepsilon_{n'}$ [63], that is

$$\mathcal{E}_{n'}\approx\varepsilon_{n'}+\Delta E_{n'}^{\bar{N}N}=-\mu_2/2n'^2+\Delta E_{n'}^{\bar{N}N}, \tag{17}$$

where μ_2 is the reduced mass of the targets $\bar{p}d$ or $\bar{p}t$ in the final channels of the reactions (3) and (4).

The idea of such a first-order approximation where pure Coulomb atomic eigenfunctions are used and the eigenvalues (atomic spectrum) are shifted, taking into account the nuclear interaction between the antiproton and the atomic nucleus, apparently goes back to Ref. [64], where low-energy scattering of antiprotons on atoms was considered. In this work we apply the few-body equations (8) and (12)–(17) with the use of an energy shift $\Delta E_{n'}^{\bar{N}N}$ in the eigenstates of $\bar{p}d$ and $\bar{p}t$. The energy shifts can be computed, for example, with the use of the well-known Deser-Goldberger-Baumann-Thirring formula [63]:

$$\Delta E_{n'}^{\bar{N}N}=-\frac{4}{n'}\frac{a_s}{B_{\bar{p}H}}\varepsilon_{n'}, \tag{18}$$

where a_s is the pure nuclear strong interaction scattering length in the $\bar{p}+H$ collision (where H is d or t), i.e. without the inclusion of Coulomb interaction between the particles, $B_{\bar{p}H}$ is the Bohr radius of deuteronium, i.e., the $\bar{p}d$ atom or the $\bar{p}t$ one. Computational details and derivations of the final equations suitable for numerical calculations can be found in the Appendix.

III. NUMERICAL RESULTS

A. Collisions between $\bar{p}$'s and muonic atoms

In this section we discus our calculations for the reactions (3) and (4). Just like in Ref. [29], in the current work we carried out numerical calculations only for the transitions to the ground state of the antiprotonic atoms, i.e., $\alpha=1s$ in Eqs. (3) and (4). In this state the size of the $\bar{p}d$ and $\bar{p}t$ atoms is about $\approx$10 fm. Thus one can expect that the contribution of the nuclear forces to the three-body scattering cross sections and rates should be significant. We assume that these reactions will be useful to study nuclear matter-antimatter interaction in future experiments.

A muon (μ^-) is $\approx$ 207 times heavier than an electron (e^-). Therefore, the muonic hydrogen atom H_μ has a very small size. As a result, in reactions (3)–(4) antiproton can very closely approach H_μ. But annihilation between $\bar{p}$ and d or t will be prevented because of the μ^- screening effect and a strong $\bar{p}$ and μ^- Coulomb repulsion. The quantum-mechanical $\bar{p}$ tunneling through the muonic-atomic orbit of H_μ is also suppressed. This effect can be seen from the following quantum-mechanical tunneling probability formula [62]:

$$B=\exp\left\{-\frac{2}{\hbar}\int_0^{\rho_0}\sqrt{2M(U(r)-E)}dr\right\}, \tag{19}$$

where B is the probability, E is the total energy in the three-body system, M is the $\bar{p}H_\mu$ reduced mass, and $U(r)$ is the interaction potential between $\bar{p}$ and H_μ:

$$U(r)=\left(\frac{1}{r}+\mu_0\right)e^{-2\mu_0 r}, \tag{20}$$

μ_0 is the muonic hydrogen reduced mass, i.e., $\mu_0\approx 207m_e$, where m_e is the electron mass. The integration in Eq. (19) can be done up to $\rho_0\approx 10$ m.a.u. One can compute the integral (19) and show that the argument of the exponent in Eq. (19) is a large number. Therefore, in the first-order approximation $\bar{p}$ tunneling can be neglected. In the case of a similar atomic system, where one has an electron e^- instead of muon, $\bar{p}$ can easily penetrate through the light e^- cloud and annihilate with the hydrogen isotopes before the three-body reaction occurs.

Figure 1 shows our results for the reaction $\bar{p}+(d\mu^-)_{1s}\to(\bar{p}d)_\alpha+\mu^-$. Specifically, panel (a) depicts our $\bar{p}$-transfer cross sections: $\sigma_{tr}(E)$. These results are shown in the framework of the $2\times1s$, $2\times(1s+2s)$, and $2\times(1s+2s+2p)$ close-coupling approximations. The contribution of the $2p$ atomic states (blue line with open circles) is large. Slow $\bar{p}$ can approach the $(d\mu)$ atom to very close distances and strongly polarize it. Therefore, the inclusion of the polarization channel in Eqs. (12)–(13) is very important. This result is in good agreement with some earlier conclusions in atomic physics [65]. Specifically, in the interaction between ions and atoms, $2p$ atomic states (channels) play a significant role in the formation of the ion+atom polarization force or polarization potential. This potential is of high importance at low- and very low-energy collisions [65].

The inclusion of the nuclear interaction between $\bar{p}$ and d increased the cross section almost three times. This is seen on Fig. 1(a) black line with open squares. The inclusion of

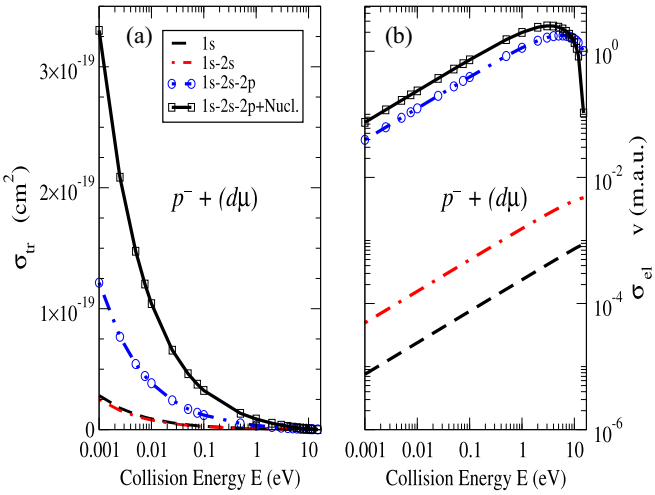

FIG. 1. (a) Three-body transfer cross section of the reaction (3) in $1s$, $1s+2s$, and $1s+2s+2p$ close-coupling approximations. (b) Elastic scattering cross section of the reaction (3) multiplied by collision velocity v. Here (m.a.u.) stands for muonic atomic units, i.e., $m_\mu = e^- = \hbar = 1$.

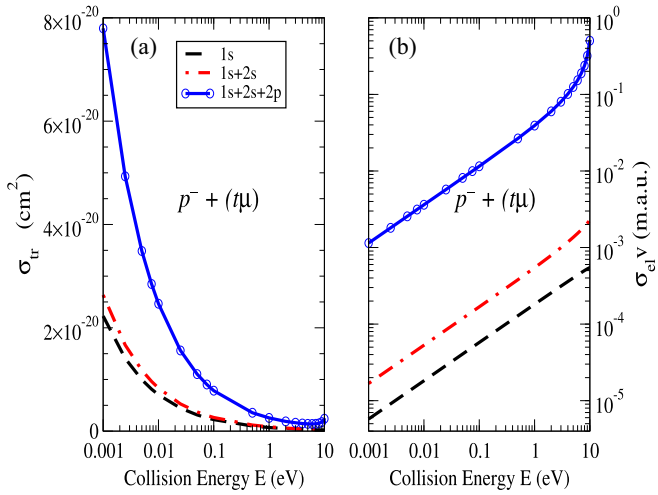

FIG. 2. (a) Three-body transfer cross section of the reaction (4) in $1s$, $1s+2s$, and $1s+2s+2p$ close-coupling approximations. (b) Elastic scattering cross section of the reaction (4) multiplied by collision velocity v in muonic atomic units, $m_\mu = e^- = \hbar = 1$.

the $\bar{p}d$ strong interaction has been done within the framework of Eqs. (16)–(18). One can find the $\bar{p}d$ atom ground-state Coulomb energy shift in Table 5.2 of Ref. [26]. The averaged experimental result has the following value:

$$\Delta E^{\bar{p}d}_{n'=1s} = 1050 \text{ eV}, \tag{21}$$

which was adopted in our work. However, the result for $\Delta E^{\bar{p}d}_{n'=1s}$ differs quite significantly from the theoretical calculations based on the three-body theory [59] and another older paper [58]. With the use of the given $\Delta E^{\bar{p}d}_{n'=1s}$ (21), one can estimate the $\bar{p}+d$ scattering length,

$$a^{\bar{p}d}_s = -\frac{B_{\bar{p}H}}{4\varepsilon_{n'=1s}} \Delta E^{\bar{p}d}_{n'=1s} = 0.682 \text{ fm}, \tag{22}$$

and compute the Coulomb energy shift for $2s$ and $2p$ states ($n' = 2$),

$$\Delta E^{\bar{p}d}_{n'=2} = 131.25 \text{ eV}. \tag{23}$$

These values have been included in Eq. (8) in our calculation of the reaction (3). In Fig. 1(b) we illustrate present results for the cross section σ_{el} multiplied by the incident velocity between the colliding particles, i.e., $\sigma_{el} v$. In this case the contribution of the $2p$ atomic states (polarization effect) is also significant, but the contribution of the strong interaction to the elastic channel is not very large.

In Fig. 2 we present our results for the reaction $\bar{p} + (t\mu^-)_{1s} \to (\bar{p}t)_\alpha + \mu^-$. This is an attractive three-charged-particle reaction with the participation of tritium. Tritium is a radioactive hydrogen isotope and it would be extremely interesting to investigate the influence of the strong interaction between $\bar{p}$ and t on the rate of the reaction (4). Also, with the study of reaction (4) it should be possible to estimate the nuclear potential between $\bar{p}$ and tritium. In Fig. 2(a) we plot the three-body transfer cross section $\sigma_{\rm tr}$ of the reaction $\bar{p} + (t\mu^-)_{1s} \to (\bar{p}t)_\alpha + \mu^-$ using $2 \times 1s$, $2 \times (1s+2s)$, and $2 \times (1s+2s+2p)$ close coupling approximations. In Fig. 2(b) we show the elastic scattering cross section multiplied by the collision velocity $\sigma_{\rm el} v$ for the process $\bar{p} + (t\mu^-)_{1s} \to \bar{p} + (t\mu^-)_{1s}$ for the three close-coupling approximations. The transfer cross section of (4) is much smaller than the corresponding transfer cross section of (3). This result agrees with the results of previous work [28].

To carry out the transfer rates of the process $\bar{p} + (t\mu^-)_{1s} \to (\bar{p}t)_\alpha + \mu^-$ one needs the nuclear energy shifts of the $(\bar{p}t)$ Coulomb levels as an input. However, to our best knowledge, these data are not available in the literature so far, i.e., there are no results for $\Delta E^{\bar{p}t}_{n'=1s}$. Some information about the $\bar{p}+t$ scattering appears in Ref. [66]. Nevertheless, we report preliminary computational results for the reaction rates of the reaction $\bar{p} + (t\mu^-)_{1s} \to (\bar{p}t)_\alpha + \mu^-$ with the use of a model approximation.

In the case of the two-particle system $(\bar{p}p)$ the energy shift is $\Delta E^{\bar{p}p}_{n'=1s} = 540$ eV. In the case of the three-particle system $\bar{p}d$, $\Delta E^{\bar{p}d}_{n'=1s} = 1050$ eV [26] (Table 5.2). Therefore, we assume that in the case of the four-particle system, i.e., $\bar{p}t$, the ground state Coulomb level energy shift due to the nuclear interaction is $\Delta E^{\bar{p}t}_{n'=1s} \approx 1575$ eV. We adopt this value and use it in our calculation of the rate of the reaction (4) with the inclusion of the strong $\bar{p}t$ interaction in the final state. As a preliminary treatment, the energy range for this calculation was only $10^{-3} \leqslant E \leqslant 2$ eV.

In these processes the inclusion of the $2p$ atomic states in the close-coupling expansion (12)-(13) is important for the transfer and for the elastic channels. In Fig. 3 we present the charge transfer rates λ for the $\bar{p}d$ and $\bar{p}t$ formation reactions, i.e.,

$$\lambda(E) = \sigma_{tr}(E) v, \tag{24}$$

where $\sigma_{tr}(E)$ is the total cross section and v is the collision velocity. These results are shown in the framework of the $2 \times 1s$, $2 \times (1s+2s)$, and $2 \times (1s+2s+2p)$ close-coupling

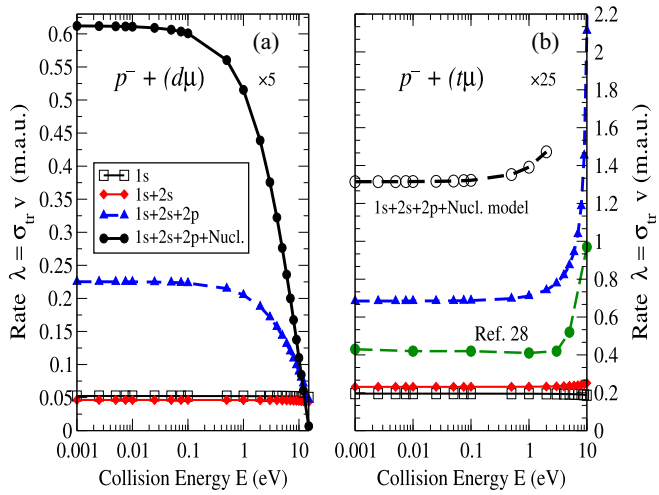

FIG. 3. (a) Three-body reaction rates for (3) in $1s$, $1s+2s$, $1s+2s+2p$ close-coupling approximations and with inclusion of the strong nuclear interaction between $\bar{p}$ and d. (b) Same as in (a) but for the reaction (4) together with the results of Ref. [28] in muonic atomic units, $m_\mu = e^- = \hbar = 1$.

approximations, viz., Eqs. (12)–(13) for (a) $\bar{p} + d\mu$ and for (b) $\bar{p} + t\mu$. The contribution of the polarization ($2p$ states) is large for both reactions. At very low energies, i.e., $E \lesssim 10^{-2}$ eV, the rates attain almost a constant value: $\lambda(E) \simeq$ const. This is in a good agreement with the general law of the quantum-mechanical rearrangement scattering theory; see for example Ref. [62]. Therefore, one can assume that the use of the six-state model is justified and acceptable in our calculations.

The energy dependence of the present rates $\lambda(E)$ agrees with the result of Ref. [28], as can be found from Fig. 3. From Figs. 3(a) and 3(b) one can conclude that the effect of the $\bar{p}d$ and $\bar{p}t$ final-state nuclear interactions on the antiproton transfer rate is significant. The effect increased the rate $\lambda(E)$ almost three times (black full line with circles). Here, as in Ref. [28], all our $\bar{p} + (d\mu^-)$ results for the reaction rates $\lambda(E)$ were multiplied by a factor of 5. The same for $\bar{p} + (t\mu^-)$: all our $\bar{p} + (t\mu^-)$ original rates, $\lambda(E)$, were multiplied by a factor of 25 in Fig. 3(b). These transfer rates attain a constant value at low energies. For the $\bar{p} + (t\mu^-)$ collision the present rates are in reasonable agreement with those obtained in Ref. [28]. In Figs. 1 and 3 we find that at low energies the contribution of the nuclear interaction could be large. This is not entirely unexpected: first, because the nuclear interaction is much larger than the atomic interaction; second, at such low energies the result is very sensitive to the model interaction used in the calculation. Only a more microscopic calculation can reveal the actual state of affairs, which is beyond the scope of the present investigation.

B. Low-energy elastic scattering: $d + (t\mu^-)_{1s}$

As a further test of our few-body approach approximation (12)-(13) we carry out additional calculations of the elastic scattering (1). This collision is of a significant interest as a Coulomb three-body problem in the muon-catalyzed fusion cycle. In the literature there are few high quality calculations of (1). These calculations are based on dissimilar quantum-mechanical methods. Here we choose two of them [67,68] for comparison with our results. As in works [67,68] we carried out computation for the so-called K_{11} matrix element, i.e., $K_{11} = \tan[\delta(\varepsilon_c)]$ for the elastic scattering (1), where $\delta(\varepsilon_c)$ is the scattering phase at the collisions energy ε_c. The set of coupled second order integral-differential Eqs. (14)–(15) has been solved numerically. As the first boundary condition we imposed

$$f_\alpha^{(1)}(\rho_1) \underset{\rho_1 \to 0}{\sim} f_{\alpha'}^{(2)}(\rho_2) \underset{\rho_2 \to 0}{\sim} 0. \tag{25}$$

We imposed a "standing wave" equation as the second boundary condition for the single open elastic scattering channel, which is described by the function $f_{1s}^{(1)}(\rho_1)$, whereas all other channels are closed:

$$f_{1s}^{(1)}(\rho_1) \underset{\rho_1 \to +\infty}{\sim} \sin\left(k_{n=1}^{(1)}\rho_1\right) + K_{11}\cos\left(k_{n=1}^{(1)}\rho_1\right),$$
$$f_{\alpha'}^{(2)}(\rho_2) \underset{\rho_2 \to +\infty}{\sim} 0. \tag{26}$$

Our calculation approach and numerical procedures are presented in the Appendix; see for example Eqs. (A20)–(A24). The authors of [67] use an adiabatic expansion approach with the use of hundreds of expansion functions in the framework of the three-body Schrödinger equation. In Ref. [68] a three-dimensional equation was numerically solved without expansion functions but only in the framework of total angular momentum $L = 0$.

In elastic scattering collisions the contribution of the polarization channels is very important. Therefore it would be interesting to check how our two-cluster equation approach works in the case of the problematic process (1). Table I shows our results for $K_{11} = \tan[\delta(\varepsilon_c)]$ together with the results of Refs. [67,68]. One can see that our simpler six-state approximation reproduces quite satisfactory results for K_{11}. Therefore, our results for K_{11} are quite sufficient to make conclusions about the validity of our computational approach and the six-state close-coupling approximation.

TABLE I. Low-energy s-wave $d + (t\mu^-)_{1s}$ elastic scattering results for $K_{11} = \tan(\delta(\varepsilon_c))$ together with the results of works [67] and [68] at kinetic energy ε_c below the $(t\mu^-)_{n=2}$ threshold.

ε_c (eV)	This work	Ref. [67]	Ref. [68]
0.01	−0.0247	−0.02384	
0.04	−0.0494	−0.0509	
0.1	−0.0784	−0.0856	−0.0875
0.3	−0.1360	−0.1627	
0.5	−0.1761	−0.2206	−0.220
1.0	−0.2509	−0.3363	−0.335

C. *p-d* exchange three-body reaction

Another intriguing system of three Coulomb particles is discussed below in this section, namely the reaction involving the massive SUSY particle X^-, i.e., the charge-exchange reaction (2). As we mentioned in the Introduction, X^- is a

TABLE II. Reaction channel total cross sections σ_t and rates λ in collision (2) at very low energies together with the corresponding results of work [10] obtained under different quantum-mechanical approximations. Here ε_c is the collision energy, v is the center-of-mass collision velocity, $\pi a_p^2 = 26.1$ b, $a_p = 28.8$ fm is the (pX^-) Bohr radius, and $\lambda = N_0 \sigma_t v$, where $N_0 = 4.25 \times 10^{22}$ cm^3 is the hydrogen density.

This work					Results from Ref. [10]		
ε_c (eV)	v (km/s)	σ_t (units of πa_p^2)	σ_t (cm^2)	λ (s^{-1})	λ^a (s^{-1})	λ^b (s^{-1})	λ^c (s^{-1})
0.0001	0.0988	4.135×10^4	107.91×10^{-20}	4.53×10^8	$\approx 0.3 \times 10^8$	$\approx 1.8 \times 10^8$	$\approx 12 \times 10^8$
0.001	0.312	1.307×10^4	34.11×10^{-20}	4.53×10^8			
0.01	0.988	0.413×10^4	10.77×10^{-20}	4.52×10^8			
0.1	3.12	1.30×10^3	3.38×10^{-20}	4.48×10^8			

[a]Screened potential approximation.
[b]Screened+dipole.
[c]Three-body Born.

hypothetical, primordial, long-lived massive particle which has its origins in the SUSY theory. The foundational idea that X^- could catalyze nuclear reactions in the BBN cycle goes back to the original publications [10,20,21,69]. This idea was subsequently developed in many stimulating studies; see for example [15,16,70]. In Ref. [71] important few-body variational calculations were performed for nuclear reaction with participation of X^- in the theory of BBN:

$$(^4\mathrm{He}\, X^-) + d \rightarrow {}^6\mathrm{Li} + X^-. \tag{27}$$

Reaction (27) could change (if X^- exist) the fundamental predictions for lithium during BBN. This is because of so-called catalytic enhancement of ^{6}Li production. In work [15] it was found that the catalytic channel is more efficient than the standard channel by factor $\approx 10^8$. It was proved in [71] with precise calculations. However, in this paper we consider another process involving X^-, namely the so-called p-d exchange reaction [10]. Apparently for the first time this reaction was mentioned in Ref. [69], and first numerical estimations of this process were done in work [10] with the following examination of the d-d nuclear reaction induced by X^-. In this paper we carry out a few-body calculation for (2) based on the set of coupled equations (8)–(9). In our computer program we basically needed just to change the masses of the particles. Our cross sections and rates are shown in Table II together with the results of work [10]. The resulting rates λ^a, λ^b, and λ^c in Table II we reproduced with the use of the corresponding total cross sections, σ_t, from Fig. 1 of Ref. [10]. The well known equation for the rate was used: $\lambda = N_0 \sigma_t v$, where N_0 is the hydrogen density and v is the initial collision velocity between d and (pX^-).

To end of section we would like to mention another three-charged-particle collision with participation of X^-. This is the reaction of the formation of $(^4\mathrm{He}\, X^-)$ with strong and long-range Coulomb interaction in the output channel:

$$^4\mathrm{He}^{++} + (pX^-) \rightarrow (^4\mathrm{He} X^-) + p. \tag{28}$$

This reaction was mentioned, for example in Ref. [16], and is related to the ^{6}Li formation problem (27). Therefore, it would be very useful and important to estimate the total cross section and the rate of the process (28). Our two component few-body approach, Eqs. (8)–(9), can be applied in the same manner as was done in paper [72].

IV. CONCLUSIONS AND OUTLOOK

In this paper, several different three-charged-particle systems were computed in a unified few-body approach. A system of coupled two-component equations (8)–(9) or (10)–(11) was applied together with a modified close-coupling approximation technique (12)–(13). The advantage of this approach over other methods is the independent formulation of the two-body targets of the reactions, for instance, $(d\mu)$ in the input channel and $(\bar{p}d)$ in the output channel in the reaction (3). This distinctive property of the coupled integral-differential equations allows us to avoid the overcompleteness problems and provide accurate three-body asymptotes for $\Psi_1(\vec{r}_{23}, \vec{\rho}_1)$ and $\Psi_2(\vec{r}_{13}, \vec{\rho}_2)$ [50].

In addition to the above, the method of the coupled equations allows us to effectively incorporate the nuclear interaction between the antiproton and deuterium nucleus in the second output channel. We treat the Coulomb and Coulomb-nuclear three-body systems with arbitrary masses, i.e., the masses of the charged particles are taken as they are. We do not apply any type of adiabatic approximations, when the dynamics of heavy and light parts of the system are separated. This makes it possible to carry out calculations of very different three-body systems both in the case of reactions and in the case of elastic scattering.

One of the main goals of this paper was to carry out a detailed few-body treatment of the heavy-charge-particle reactions (3) and (4) at low energies and investigate the influence of the strong nuclear interaction on the final state of these reactions, i.e., the influence of the $\bar{p}d$ and $\bar{p}t$ short-range nuclear forces on the output parameters of (3) and (4). In the case of the reaction (3) we demonstrated that this influence is quite significant: up to 275%. Therefore, one can conclude that the three-body reaction can be considered as a possible candidate for future experiments with participation of low-energy antiprotons and muons in order to produce the antiprotonic hydrogen atom $(\bar{p}d)$ and study the nuclear interaction between $\bar{p}$ and d at low energies. In regard to the very interesting $(\bar{p}t)$ system we carried only preliminary estimations of the influence of the strong $\bar{p}t$ forces on the reaction outputs. It was also found that the effect is significant.

There is another useful point related to the reactions (3) and (4). It concerns the problem of the long-range part of the strong $\bar{N}N$ interaction [22]. We assume that these forces and,

for instance, isospin mixing effects can manifest themselves in the antiprotonic atoms' $(\bar{p}d)$ and $(\bar{p}t)$ radiative annihilation [73]. In the case of the low-energy elastic scattering (1) we obtained satisfactory results for the tangent of the scattering phase $\delta(\varepsilon_c)$, i.e., K_{11}. One can see from Table I that our six-state $1s+2s+2p$ close-coupling approximation works very well, especially at very low energies.

Regarding the charge-exchange reaction (2) involving the superheavy X^- particle we have also applied the six-state approximation. The strong polarization forces have been included in these calculations. As can be seen from Table II, our results are close to those of work [10] performed in the *screened + dipole* approximation. This fact allows us to hope that it is possible to continue such calculations (as in the current work) and apply the few-body dynamic equations to the Coulombic reaction (28) with subsequent consideration of the importance, in the catalyzed BBN theory [15,71], of the lithium formation nuclear reaction (27).

ACKNOWLEDGMENTS

S.K.A. acknowledges support by Conselho Nacional de Desenvolvimento Científico e Tecnológico (CNPq), Brazil under Grant No. 301324/2019-0.

APPENDIX

It would be useful to rewrite Eqs. (8) and (9) in the following compact form using notations of Eq. (5):

$$\left(E+\frac{1}{2M_k}\triangle_{\vec{\rho}_k}+\frac{1}{2\mu_j}\triangle_{\vec{r}_{j3}}-V_{j3}\right)\Psi_i(\vec{r}_{j3},\vec{\rho}_k)$$
$$=(V_{j3}+V_{jk})\Psi_{i'}(\vec{r}_{k3},\vec{\rho}_j), \tag{A1}$$

where $i\neq i'=1,2$, $M_j^{-1}=m_j^{-1}+(m_3+m_k)^{-1}$, and $\mu_j^{-1}=m_3^{-1}+m_k^{-1}$, where $j\neq k=1,2$. To separate the radial and angular variables, we expand the wave function components Ψ_i over the bipolar harmonics:

$$\{Y_\lambda(\hat{\rho})\otimes Y_l(\hat{r})\}_{LM}=\sum_{\mu m}C^{LM}_{\lambda\mu lm}Y_{\lambda\mu}(\hat{\rho})Y_{lm}(\hat{r}), \tag{A2}$$

where $C^{LM}_{\lambda\mu lm}$ are Clebsh-Gordon coefficients and Y_{lm} are spherical harmonics [55,74]. If we substitute theexpansion of the wave-function component,

$$\Psi_i(\vec{r}_{j3},\vec{\rho}_k)=\sum_{LM\lambda l}\Phi^i_{LM\lambda l}(\rho_k,r_{j3})\{Y_\lambda(\hat{\rho}_k)\otimes Y_l(\hat{r}_{j3})\}_{LM},$$

into (A1), multiply by the appropriate biharmonic functions, and integrate over the corresponding angular coordinates of the vectors $\vec{r}_{j3}$ and $\vec{\rho}_k$, we obtain the following set of integral-differential equations for the case of central potentials:

$$\left[E+\frac{1}{2M_k\rho_k^2}\left\{\frac{\partial}{\partial\rho_k}\left(\rho_k^2\frac{\partial}{\partial\rho_k}\right)-\lambda(\lambda+1)\right\}+\frac{1}{2\mu_j r_{j3}^2}\left\{\frac{\partial}{\partial r_{j3}}\left(r_{j3}^2\frac{\partial}{\partial r_{j3}}\right)-l(l+1)\right\}-V_{j3}\right]\Phi^i_{LM\lambda l}(\rho_k,r_{j3})$$
$$=\int d\hat{\rho}_k\int d\hat{r}_{j3}\sum_{\lambda' l'}W^{(ii')LM}_{\lambda l\lambda' l'}\Phi^{i'}_{LM\lambda' l'}(\rho_j,r_{k3}), \tag{A3}$$

where

$$W^{(ii')LM}_{\lambda l\lambda' l'}=\{Y_\lambda(\hat{\rho}_k)\otimes Y_l(\hat{r}_{j3})\}^*_{LM}(V_{j3}+V_{jk})\{Y_{\lambda'}(\hat{\rho}_j)\otimes Y_{l'}(\hat{r}_{k3})\}_{LM}. \tag{A4}$$

One-dimensional equations, convenient for numerical calculations, are obtained if we apply, for example, a modified close-coupling approach, which consists of expanding each component of the wave function $\Psi_i(\vec{r}_{j3},\vec{\rho}_k)$ over the eigenfunctions of the following subsystem Hamiltoninans:

$$\hat{h}_{j3}=-\frac{1}{2\mu_j}\nabla^2_{\vec{r}_{j3}}+V_{j3}(\vec{r}_{j3}). \tag{A5}$$

Therefore, we use the following expansion over a complete set of orthogonal atomic functions:

$$\Phi^i_{LM\lambda l}(\rho_k,r_{j3})=\frac{1}{\rho_k}\sum_n f^{(i)LM}_{nl\lambda}(\rho_k)R^{(i)}_{nl}(r_{j3}), \tag{A6}$$

where functions $R^{(i)}_{nl}(r_{j3})$ with energy E^i_n are defined by the equation

$$\left[E^i_n+\frac{1}{2\mu_j r_{j3}^2}\left\{\frac{\partial}{\partial r_{j3}}\left(r_{j3}^2\frac{\partial}{\partial r_{j3}}\right)-l(l+1)\right\}-V_{j3}\right]R^{(i)}_{nl}(r_{j3})=0. \tag{A7}$$

Now by substituting Eq. (A6) into (A3), multiplying by the corresponding functions $R^{(i)}_{nl}(r_{j3})$ and integrating over $r^2_{j3}dr_{j3}$, we obtain the following set of integral-differential equations for the unknown functions $f^{(i)}_{nl\lambda}(\rho_k)$:

$$2M_k(E-E^i_n)f^{(i)}_\alpha(\rho_k)+\left[\frac{\partial^2}{\partial\rho_k^2}-\frac{\lambda(\lambda+1)}{\rho_k^2}\right]f^{(i)}_\alpha(\rho_k)=2M_k\sum_\alpha\int_0^\infty dr_{j3}r^2_{j3}\int d\hat{r}_{j3}\int d\hat{\rho}_k\rho_k Q^{ii'}_{\alpha\alpha'}\rho_j f^{(i')}_{\alpha'}(\rho_j), \tag{A8}$$

where $Q^{ii'}_{\alpha\alpha'}=R^{(i)}_{nl}(r_{j3})W^{(ii')LM}_{\lambda l\lambda' l'}R^{(i')}_{n'l'}(r_{k3})$. In Eq. (A8) and in the following, $\alpha\equiv nl\lambda$ ($\alpha'\equiv n'l'\lambda'$), and the redundant label LM will be omitted. Equation (A8) is still not one dimensional, because α and α' involve different frames of the Jacobi coordinates,

$$\vec{\rho}_j=\vec{r}_{j3}-\beta_k\vec{r}_{k3},\quad \vec{r}_{j3}=\frac{1}{\gamma}(\beta_k\vec{\rho}_k+\vec{\rho}_j),\quad \vec{r}_{jk}=\frac{1}{\gamma}(\sigma_j\vec{\rho}_j-\sigma_k\vec{\rho}_k), \tag{A9}$$

with the following mass coefficients:

$$\beta_k=m_k/(m_3+m_k),\quad \sigma_k=1-\beta_k,\quad \gamma=1-\beta_k\beta_j,\quad j\neq k=1,2. \tag{A10}$$

It clearly demonstrates that the modulus of $\vec{\rho}_j$ depends on two vectors, over which integration on the right-hand side of Eq. (A8) is performed. One can see from Eq. (20) $\vec{\rho}_j=\gamma\vec{r}_{j3}-\beta_k\vec{\rho}_k$. Therefore, in order to obtain a set of one-dimensional integral-differential equations, corresponding to Eqs. (A8), we will carry out integration over variables $\{\vec{\rho}_j,\hat{\rho}_k\}$ rather than $\{\vec{r}_{j3},\hat{\rho}_k\}$. The Jacobian of this transformation is $J=\gamma^{-3}$. Thus, we obtain the following set of one-dimensional integral-differential equations:

$$2M_k\big(E-E^i_n\big)f^{(i)}_\alpha(\rho_k)+\left[\frac{\partial^2}{\partial\rho_k^2}-\frac{\lambda(\lambda+1)}{\rho_k^2}\right]f^{(i)}_\alpha(\rho_k)=\frac{M_k}{\gamma^{-3}}\sum_{\alpha'}\int_0^\infty d\rho_j S^{ii'}_{\alpha\alpha'}(\rho_j,\rho_k)f^{(i')}_{\alpha'}(\rho_j), \tag{A11}$$

where

$$S^{ii'}_{\alpha\alpha'}(\rho_j,\rho_k)=2\rho_j\rho_k\int d\hat{\rho}_j\int d\hat{\rho}_k R^{(i)}_{nl}(r_{j3})\{Y_\lambda(\hat{\rho}_k)\otimes Y_l(\hat{r}_{j3})\}^*_{LM}(V_{j3}+V_{jk})\{Y_{\lambda'}(\hat{\rho}_j)\otimes Y_{l'}(\hat{r}_{k3})\}_{LM}R^{(i')}_{n'l'}(r_{k3}). \tag{A12}$$

In Ref. [54] it was shown that the fourfold multiple integration in Eqs. (A12) leads to a one-dimensional integral, and the expression (A12) could be determined for any orbital momentum value L as

$$\begin{aligned}S^{ii'}_{\alpha\alpha'}(\rho_j,\rho_k)=&\frac{4\pi[(2\lambda+1)(2\lambda'+1)]^{\frac{1}{2}}}{2L+1}\int_0^\pi d\omega\sin\omega\rho_j\rho_k R^{(i)}_{nl}(r_{j3})[V_{j3}(r_{j3})+V_{jk}(r_{jk})]R^{(i')}_{n'l'}(r_{k3})\\&\times\sum_{mm'}D^L_{mm'}(0,\omega,0)C^{Lm}_{\lambda 0lm}C^{Lm'}_{\lambda' 0l'm'}Y_{lm}(\nu_j,\pi)Y^*_{l'm'}(\nu_k,\pi),\end{aligned} \tag{A13}$$

where $D^L_{mm'}(0,\omega,0)$ are Wigner functions, ω is the angle between $\vec{\rho}_j$ and $\vec{\rho}_k$, ν_j is the angle between $\vec{r}_{k3}$ and $\vec{\rho}_j$, and ν_k is the angle between $\vec{r}_{j3}$ and $\vec{\rho}_k$. As a result we obtain an infinite set of one-dimensional coupled integral-differential equations for the unknown functions $f^1_\alpha(\rho_1)$ and $f^2_{\alpha'}(\rho_2)$ [54]:

$$\begin{aligned}\left[\big(k^i_n\big)^2+\frac{\partial^2}{\partial\rho_i^2}-\frac{\lambda(\lambda+1)}{\rho_i^2}\right]f^{(i)}_\alpha(\rho_i)=&\sum_{\alpha'}\int_0^\infty d\rho_{i'}f^{(i')}_{\alpha'}(\rho_{i'})\sqrt{\frac{(2\lambda+1)(2\lambda'+1)}{(2L+1)^2}}\int_0^\pi d\omega\sin\omega R^{(i)}_{nl}(r_{i'3})\\&\times g_i(V_{i'3}(r_{i'3})+V_{ii'}(r_{ii'}))R^{(i')}_{n'l'}(r_{i3})\rho_{i'}\rho_i\sum_{mm'}D^L_{mm'}(0,\omega,0)C^{Lm}_{\lambda 0lm}C^{Lm'}_{\lambda' 0l'm'}\\&\times Y_{lm}(\nu_i,\pi)Y^*_{l'm'}(\nu_{i'},\pi),\end{aligned} \tag{A14}$$

where L is the total angular momentum of the three-body system and $\alpha\equiv(nl\lambda)$ are quantum numbers of a three-body state and

$$g_i=\frac{4\pi M_i}{\gamma^3},\quad k^i_n=\sqrt{2M_i\big(E-E^{i'}_n\big)},\quad \gamma=1-\frac{m_im_{i'}}{(m_i+m_3)(m_{i'}+m_3)},\quad i\neq i'=1,2. \tag{A15}$$

where $M_1=m_1(m_2+m_3)/(m_1+m_2+m_3)$, $M_2=m_2(m_1+m_3)/(m_1+m_2+m_3)$, are the reduced masses. We note the useful relations $\sin\nu_i=\rho_{i'}\sin\omega/\gamma r_{i'3}$ and $\cos\nu_i=(\beta_i\rho_i+\rho_{i'}\cos\omega)/\gamma r_{i'3}$.

In the case of reactions (2), (3), and (4), we use the following boundary conditions. First, we impose

$$f^{(i)}_{nl}(0)\sim 0, \tag{A16}$$

and as a second step we apply the well known $\hat{K}$-matrix formalism. This method has already been applied for the solution of three-body problems in the framework of a coordinate-space equation [67,68]. For our three-body reaction problems with $i+(j3)$ as the initial state in the asymptotic region it considers two solutions to Eq. (A14) satisfying the following boundary

conditions:

$$f_{1s}^{(i)}(\rho_i) \underset{\rho_i\to+\infty}{\sim} \sin\left(k_{n=1}^{(i)}\rho_i\right) + K_{ii}\cos\left(k_{n=1}^{(i)}\rho_i\right),$$
$$f_{1s}^{(j)}(\rho_j) \underset{\rho_j\to+\infty}{\sim} \sqrt{v_i/v_j}K_{ij}\cos\left(k_{n=1}^{(j)}\rho_j\right), \tag{A17}$$

where $(i \neq j = 1, 2)$, K_{ij} are the appropriate coefficients, and v_i is the velocity in channel i. With the following change of the variables in the Eq. (A14):

$$\mathrm{f}_{1s}^{(i)}(\rho_i) = f_{1s}^{(i)}(\rho_i) - \sin\left(k_{n=1}^{(i)}\rho_i\right), \tag{A18}$$

we get two sets of inhomogeneous equations which we solve numerically. The coefficients K_{ij} can be obtained from a numerical solution of the coupled equations. The cross sections are given by the following formula:

$$\sigma_{ij} = \frac{4\pi}{k_{n=1}^{(i)2}}\left|\frac{\hat{K}}{1-\mathrm{i}\hat{K}}\right|^2 = \frac{4\pi}{k_{n=1}^{(i)2}}\frac{\delta_{ij}D^2 + K_{ij}^2}{(D-1)^2 + (K_{11}+K_{22})^2}, \tag{A19}$$

where $(i, j = 1, 2)$ refer to the two channels, $D = K_{11}K_{22} - K_{12}K_{21}$, and i is the imaginary unit.

In order to compute the reaction cross sections, i.e., Eq. (A19), we have to solve numerically the set of integral-differential equations (A14). The angular integrals in Eq. (A13) are independent of energy E, therefore we needed to compute them only once. The subintegral expressions in (A13) have a complex dependence on the Jacobi coordinates ρ_i and $\rho_{i'}$. To calculate $S_{\alpha\alpha'}^{(ii')}(\rho_i, \rho_{i'})$ at different values of ρ_i and $\rho_{i'}$ an adaptable computer algorithm was applied together with the following mathematical substitution: $\cos\omega = (x^2 - \beta_i^2\rho_i^2 - \rho_{i'}^2)/(2\beta_i\rho_i\rho_{i'})$. Therefore, the angle dependent part of Eq. (A13) can be written as the following one-dimensional integral:

$$S_{\alpha\alpha'}^{(ii')}(\rho_i, \rho_{i'}) = \frac{4\pi}{\beta_i}\frac{[(2\lambda+1)(2\lambda'+1)]^{\frac{1}{2}}}{2L+1}\int_{|\beta_i\rho_i-\rho_{i'}|}^{(\beta_i\rho_i+\rho_{i'})} dx R_{nl}^{(i)}(x)\left[-1 + \frac{x}{r_{ii'}(x)}\right]R_{n'l'}^{(i')}(r_{i3}(x))$$
$$\times \sum_{mm'} D_{mm'}^{L}(0, \omega(x), 0)C_{\lambda 0lm}^{Lm}C_{\lambda' 0l'm'}^{Lm'}Y_{lm}(v_i(x), \pi)Y_{l'm'}^{*}(v_{i'}(x), \pi). \tag{A20}$$

A special adaptive FORTRAN program was used in order to carry out the angle integration in (A20).

The set of truncated integral-differential equations (A14) is solved by a discretization procedure; i.e., on the right side of the equations the integrals over ρ_1 and ρ_2 are replaced by sums using the trapezoidal rule, and the second-order partial derivatives on the left side are discretized using a three-point rule [74]. As a result a set of linear equations for the unknown coefficients $f_\alpha^{(i)}(k)$ $(k = 1, N_p)$ can be derived:

$$\left[k_n^{(1)2} + D_{ij}^2 - \frac{\lambda(\lambda+1)}{\rho_{1i}^2}\right]f_\alpha^{(1)}(i) - \frac{M_1}{\gamma^3}\sum_{\alpha'=1}^{N_s}\sum_{j=1}^{N_p} w_j S_{\alpha\alpha'}^{(12)}(\rho_{1i}, \rho_{2j})f_{\alpha'}^{(2)}(j) = 0, \tag{A21}$$

$$-\frac{M_2}{\gamma^3}\sum_{\alpha=1}^{N_s}\sum_{j=1}^{N_p} w_j S_{\alpha'\alpha}^{(21)}(\rho_{2i}, \rho_{1j})f_\alpha^{(1)}(j) + \left[k_{n'}^{(2)2} + D_{ij}^2 - \frac{\lambda'(\lambda'+1)}{\rho_{2i}^2}\right]f_{\alpha'}^{(2)}(i) = B_{\alpha'}^{21}(i). \tag{A22}$$

Here: coefficients w_j are weights of the integration points ρ_{1i} and ρ_{2i} $(i = 1, N_p)$, N_s is the number of quantum states which are taken into account in the expansion (A6). Further, D_{ij}^2 is the three-point numerical approximation for the second-order differential operator: $D_{ij}^2 f_\alpha(i) = [f_\alpha(i-1)\delta_{i-1,j} - 2f_\alpha(i)\delta_{i,j} + f_\alpha(i+1)\delta_{i+1,j}]/\Delta$, where Δ is a step of the grid $\Delta = \rho_{i+1} - \rho_i$. The vector $B_{\alpha'}^{21}(i)$ is

$$B_{\alpha'}^{(21)}(i) = M_2/\gamma^3\sum_{j=1}^{N_p} w_j S_{\alpha' 1s0}^{(21)}(i, j)\sin\left(k_{n=1}^{(j)}\rho_j\right), \tag{A23}$$

and in symbolic-operator notation the set of linear Eqs. (A21)–(A22) has the following form [54]:

$$\sum_{\alpha'=1}^{2\times N_s}\sum_{j=1}^{N_p}\mathbf{A}_{\alpha\alpha'}(i, j)\vec{f}_{\alpha'}(j) = \vec{b}_\alpha(i). \tag{A24}$$

The discretized equations are subsequently solved by the Gauss elimination procedure. The second-order differential operators produce three diagonal submatrices. Also, from Eqs. (A21)–(A22) one can see that the matrix $\mathbf{A}$ should have a so-called block-structure. There are four main blocks in the matrix: two of them related to the differential operators and other two to the integral operators. Each of these blocks should have sub-blocks depending on the quantum numbers $\alpha = nl\lambda$ and $\alpha' = n'l'\lambda'$.

[1] *Recent Progress in Few-Body Physics*, Proceedings of 22nd International Conference on Few-Body Problems in Physics, edited by N. A. Orr, M. Ploszajczak, F. M. Marqués, and J. Carbonell, Springer Proceedings in Physics Vol. 238 (Springer, Berlin, 2020).
[2] R. Ya. Kezerashvili, Few-Body Syst. **60**, 52 (2019).
[3] R. Combescot, Phys. Rev. X **7**, 041035 (2017).
[4] H.-W. Hammer, A. Nogga, and A. Schwenk, Rev. Mod. Phys. **85**, 197 (2013).
[5] L. I. Ponomarev, Contemp. Phys. **31**, 219 (1990).
[6] T. Yamashita, Y. Kino, K. Okutsu, S. Okada, and M. Sato, Sci. Rep. **12**, 6393 (2022).
[7] S. Liu, D. Ye, and J. Liu, Phys. Rev. C **106**, 064611 (2022).
[8] M. Pospelov and J. Pradler, Annu. Rev. Nucl. Part. Sci. **60**, 539 (2010).
[9] G. J. Mathews, M. Kusakabe, and T. Kajino, Int. J. Mod. Phys. E **26**, 1741001 (2017).
[10] M. Sawicki, M. Gajda, D. Harley, and J. Rafelski, Phys. Rev. A **44**, 4345 (1991).
[11] G. Aad *et al.* (ATLAS Collaboration), Phys. Rev. D **101**, 032009 (2020).
[12] A. M. Sirunyan *et al.* (CMS Collaboration), Phys. Lett. B **790**, 140 (2019).
[13] J. Alimena *et al.*, J. Phys. G: Nucl. Part. Phys. **47**, 090501 (2020).
[14] A. M. Sirunyan *et al.* (CMS Collaboration), Eur. Phys. J. C **80**, 189 (2020).
[15] M. Pospelov, Phys. Rev. Lett. **98**, 231301 (2007).
[16] K. Jedamzik and M. Pospelov, New J. Phys. **11**, 105028 (2009).
[17] M. Kusakabe, G. J. Mathews, and T. Kajino, Int. J. Mod. Phys. E **26**, 1741004 (2017).
[18] K. Ishida, K. Nagamine, T. Matsuzaki, and N. Kawamura, J. Phys. G: Nucl. Part. Phys. **29**, 2043 (2003).
[19] R. N. Boyd, K. Takahashi, R. J. Perry, and T. A. Miller, Science **244**, 1450 (1989).
[20] A. De Rujula, S. L. Glashow, and U. Sarid, Nucl. Phys. B **333**, 173 (1990).
[21] S. Dimopoulos, D. Eichler, R. Esmailzadeh, and G. D. Starkman, Phys. Rev. D **41**, 2388 (1990).
[22] W. W. Buck, C. B. Dover, and J. M. Richard, Ann. Phys. (NY) **121**, 47 (1979).
[23] T. Hippchen, J. Haidenbauer, K. Holinde, and V. Mull, Phys. Rev. C **44**, 1323 (1991).
[24] C. J. Batty, E. Friedman, and A. Galb, Phys. Rep. **287**, 385 (1997).
[25] E. Klempt, C. Batty, and J.-M. Richard, Phys. Rep. **413**, 197 (2005).
[26] E. Klempt, F. Bradamante, A. Martin, and J.-M. Richard, Phys. Rep. **368**, 119 (2002).
[27] D. Gotta, Prog. Part. Nucl. Phys. **52**, 133 (2004).
[28] A. Igarashi and N. Toshima, Eur. Phys. J. D **46**, 425 (2008).
[29] R. A. Sultanov, D. Guster, and S. K. Adhikari, Atoms **6**, 18 (2018).
[30] L.-Y. Dai, J. Haidenbauer, and U.-G. Meißner, J. High Energy Phys. 07 (2017) 078.
[31] A. Knecht, A. Skawran, and S. M. Vogiatzi, Eur. Phys. J. Plus **135**, 777 (2020).
[32] C. Ji, S. Bacca, N. Barnea, O. J. Hernandez, and N. Nevo Dinur, J. Phys. G: Nucl. Part. Phys. **45**, 093002 (2018).
[33] J. Eschke, J. Phys. G: Nucl. Part. Phys. **31**, S967 (2005).
[34] J. Steinheimer *et al.*, J. Phys. G: Nucl. Part. Phys. **37**, 094026 (2010).
[35] J.-M. Richard, Front. Phys. **8**, 6 (2020).
[36] M. Ahmadi *et al.*, Nature (London) **557**, 71 (2018).
[37] M. Hori, Phil. Trans. R. Soc. A **376**, 20170270 (2018).
[38] S. Jonsell, Phil. Trans. R. Soc. A **376**, 20170271 (2018).
[39] T. Yamashita, Y. Kino, E. Hiyama, S. Jonsell, and P. Froelich, Phys. Rev. A **105**, 052812 (2022).
[40] R. Pohl *et al.*, Nature (London) **466**, 213 (2010).
[41] S. Schmidt *et al.*, J. Phys.: Conf. Ser. **1138**, 012010 (2018).
[42] A. Antognini, F. Kottmann, and R. Pohl, SciPost Phys. Proc. **5**, 021 (2021).
[43] A. Skawran *et al.*, IL Nuovo Cimento **42 C**, 125 (2019).
[44] A. Antognini, F. Hagelstein, and V. Pascalutsa, Annu. Rev. Nucl. Part. Sci. **72**, 389 (2022).
[45] Y. Yamazaki and S. Ulmer, Ann. Phys. (Berlin) **525**, 493 (2013).
[46] M. S. Safronova, D. Budker, D. DeMille, D. F. Jackson Kimball, A. Derevianko, and C. W. Clark, Rev. Mod. Phys. **90**, 025008 (2018).
[47] W. Tobocman, Phys. Rev. C **9**, 2466 (1974); **10**, 60 (1974); **11**, 43 (1975); **12**, 741 (1975).
[48] Y. Hahn and K. Watson, Phys. Rev. A **5**, 1718 (1972).
[49] Y. Hahn, D. J. Kouri, and F. S. Levin, Phys. Rev. C **10**, 1615 (1974).
[50] Y. Hahn, Phys. Rev. C **16**, 2449 (1977).
[51] F. S. Levin, Phys. Rev. C **21**, 2199 (1980).
[52] Y. Hahn, Phys. Lett. B **97**, 1 (1980).
[53] Y. Hahn, Nucl. Phys. A **389**, 1 (1982).
[54] R. A. Sultanov and D. Guster, J. Comput. Phys. **192**, 231 (2003); J. Phys. B: At. Mol. Opt. Phys. **46**, 215204 (2013).
[55] D. A. Varshalovich, A. N. Moskalev, and V. L. Khersonskii, *Quantum Theory of Angular Momentum* (World Scientific, Singapore, 1988).
[56] C. B. Dover and J.-M. Richard, Phys. Rev. C **21**, 1466 (1980).
[57] C. B. Dover and J.-M. Richard, Phys. Rev. C **25**, 1952 (1982).
[58] S. Wycech, A. M. Green, and J. A. Niskanen, Phys. Lett. B **152**, 308 (1985).
[59] G. P. Latta and P. C. Tandy, Phys. Rev. C **42**, R1207 (1990).
[60] D. R. Entem and F. Fernandez, Phys. Rev. C **73**, 045214 (2006).
[61] Y. Yan, K. Khosonthongkee, C. Kobdaj *et al.*, Phys. Lett. B **659**, 555 (2008); **665**, 425 (2008).
[62] L. D. Landau and E. M. Lifshitz, *Quantum-Mechanics (Non-relativistic Theory)*, Course of Theoretical Physics Vol. 3, 3rd ed. (Butterworth-Heinemann, Oxford, 2003).
[63] S. Deser, M. L. Goldberger, K. Baumann, and W. Thirring, Phys. Rev. **96**, 774 (1954).
[64] O. Dumbrajs, Phys. Rev. A **32**, 637 (1985).
[65] N. F. Mott and H. S. W. Massey, *The Theory of Atomic Collisions*, 3rd ed. (Clarendon Press, Oxford, 1965).
[66] L. A. Kondratyuk and M. Z. Shmatikov, Sov. J. Nucl. Phys. **38**, 216 (1983).
[67] C. Chiccoli *et al.*, Muon Catalyzed Fusion **7**, 87 (1992).
[68] A. A. Kvitsinsky, C.-Y. Hu, and J. S. Cohen, Phys. Rev. A **53**, 255 (1996).
[69] B. L. Ioffe, L. B. Okun', M. A. Shifman, and M. B. Voloshin, Acta Phys. Pol. B **12**, 229 (1981).
[70] A. Kamada, N. Yoshida, K. Kohric, and T. Takahashie, J. Cosmol. Astropart. Phys. **3**, 008 (2013).

[71] K. Hamaguchi, T. Hatsuda, M. Kamimura, Y. Kino, and T. T. Yanagida, Phys. Lett. B **650**, 268 (2007).

[72] R. A. Sultanov and S. K. Adhikari, J. Phys. B **32**, 5751 (1999).

[73] T. Gutsche, R. V. Mau, M. Strohmeier-Prešiček, and A. Faessler, Phys. Rev. C **59**, 630 (1999).

[74] M. Abramowitz and I. A. Stegun, *Handbook of Mathematical Functions: With Formulas, Graphs, and Mathematical Tables* (Dover, New York, 1965).